Relationship between air and soil temperature trends and periodicities in the permafrost regions of Russia

Svetlana M. Chudinova,[1] Oliver W. Frauenfeld,[2] Roger G. Barry,[2] Tingjun Zhang,[2] and Victor A. Sorokovikov[1]

Received 27 May 2005; revised 18 January 2006; accepted 6 February 2006; published 17 May 2006.

[1] Soil temperature is an important indicator of frozen ground status, driven at least partly by air temperature variability. In this study we apply singular spectrum analysis (SSA) to detect trends and oscillations in annual and seasonal time series of surface air temperature (SAT) and soil temperature (ST). We investigate soil temperatures at depths of 0.4, 1.6, and 3.2 m for five permafrost-occupied regions in Russia. We use SAT data for 1902–1995 and ST data for 1960–1990. The trends show an increase in annual SAT and ST from the end of the 1960s across all five regions, and this warming exceeds that of the preceding period in the Central Siberian Plateau and Transbaikalia. Oscillations in annual SAT and ST time series are coincident in the West Siberian Plain (7.7 year period) and in the western Central Siberian Plateau and Transbaikalia (2.7 year period). In general, on a seasonal basis, 2–3 year oscillations in ST and SAT are coincident during winter, spring, and autumn across the regions and are also evident in the annual ST time series in the Central Siberian Plateau and Transbaikalia. We also find a decadal oscillation (9.8 year period), which is coincident for winter SAT and ST, over the western Central Siberian Plateau only. Although summer SAT and ST oscillations (5–8 year periods) are coincident for all investigated territories (except to the east of the Lena River), in the annual ST time series they are identified only for the West Siberian Plain. We document the degree to which SAT controls ST in each region and explore the causative factors for some of the dominant periods. The maximum effect of SAT increases on permafrost may be observed in the Central Siberian Plateau and Transbaikalia, while elsewhere the observed ST increases do not threaten permafrost areas.

Citation: Chudinova, S. M., O. W. Frauenfeld, R. G. Barry, T. Zhang, and V. A. Sorokovikov (2006), Relationship between air and soil temperature trends and periodicities in the permafrost regions of Russia, *J. Geophys. Res.*, *111*, F02008, doi:10.1029/2005JF000342.

1. Introduction

[2] Soil temperature (ST) is an important indicator of permafrost status. Knowledge of long- and short-term fluctuations in ST time series in the upper (0–3.0 m) soil layer allow us to assess changes in the depth of the active layer and predict the future status of the upper boundary of permafrost. ST and freeze/thaw status are especially important for Russia, where permafrost occupies approximately 60% of the area [*Yershov*, 1998].

[3] Recent investigations show that surface air temperature (SAT) increases in recent decades over the Russian territory are neither spatially nor temporally uniform. *Fallot et al.* [1997] found significant positive trends in winter temperatures across much of the former Soviet Union in the past 50 years. Similarly, *Serreze et al.* [2000] document increased winter temperatures over widespread areas in Eurasia, but warming was greatest for 1966–1995 in the West Siberian Plain during spring and summer. During the second half of the 20th century, air temperatures in the West Siberian Plain and western Central Siberian Plateau correlated closely with average global temperature changes [*Anisimov*, 2001], and *Frey and Smith* [2003] identified recent strong springtime warming at nine meteorological stations in West Siberia.

[4] Because of a strong correspondence between SAT and ST, changes in ST should be similarly nonuniform across Russia. However, ST also depends on numerous environmental factors such as snow depth, vegetation canopy, soil moisture and texture, organic matter accumulation, freeze/thaw, and hydrologic processes. A number of studies have suggested that ground and air temperature track each other at both long timescales (several centuries) [e.g., *Huang et al.*, 2000; *Harris and Chapman*, 2001; *Beltrami and Bourlon*, 2004; *Pollack and Smerdon*, 2004], and annual to century scales [e.g., *Putman and Chapman*, 1996; *Majorowicz and Skinner*, 1997; *Beltrami et al.*, 2005]. On the other hand, other research has shown that the relationship between SAT and ST is more complicated because of

[1] Institute of Physicochemical and Biological Problems in Soil Science, Russian Academy of Sciences, Pushchino, Russia.
[2] Cooperative Institute for Research in Environmental Sciences, National Snow and Ice Data Center, University of Colorado, Boulder, Colorado, USA.

0148-0227/06/2005JF000342

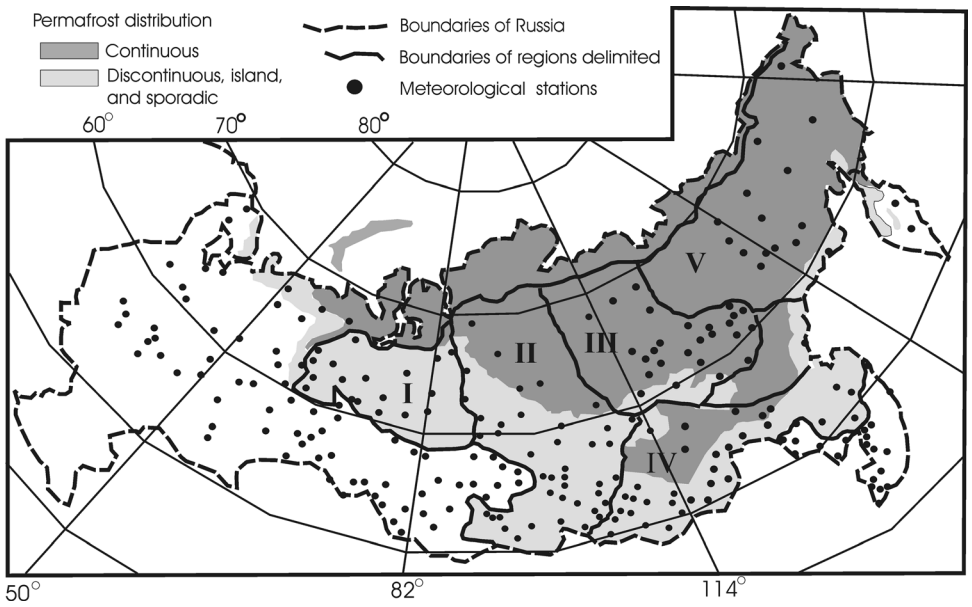

Figure 1. Location of the available meteorological stations and regions investigated (I–V).

the influence of the many other climatic factors. For example, snow cover has been demonstrated to account for the differences between SAT and ST during the cold season [*Mann and Schmidt*, 2003; *González-Rouco et al.*, 2003; *Bartlett et al.*, 2005]. *Skinner and Majorowicz* [1999] suggest that for several provinces in Canada, the difference in SAT and ST increases during the twentieth century is related to land use and further show that the interannual ST and SAT connection is stronger in the summer half of the year than in winter.

[5] *Gilichinsky et al.* [1998] showed an inverse relationship between ST and SAT and, similarly, *Zhang et al.* [2001] found that in spite of increased summer SAT at Irkutsk, summer ST decreased due to abundant precipitation. However, the magnitude of the winter ST increase was 3°–5°C higher than the winter SAT increase, due primarily to changes in snow cover conditions. *Chudinova et al.* [2001] analyzed linear trends of monthly SAT, ST, and snow depth (for 1966–1990) at 11 meteorological stations in the northern Russian Plain and found that, due to the insulation effect of snow cover, increases in winter SAT do not affect ST. Instead, summer increases in ST were related to a strong rise in SAT at the beginning of the warm season. Prediction of potential changes in the soil thermal regime at the regional scale therefore requires an understanding of the complex interactions between ST and SAT in high-latitude regions.

[6] An important and unresolved question that thus still remains, especially in light of the heightened interest in global climate change, is what drives observed ST changes in regions characterized by seasonally and permanently frozen ground? This outstanding issue is difficult to address, partly due to lack of adequate data for high-latitude regions. Subsurface temperatures from deep boreholes (200–600 m) can be used to reconstruct century- to millennium-scale fluctuations in 0–3.0 m ST, and can serve as proxies for fluctuations in SAT [see, e.g., *Lewis*, 1992; *Pollack and Chapman*, 1993; *Vasseur and Mareschal*, 1993; *Beltrami and Chapman*, 1994]. Furthermore, approaches for reconstructing ground surface temperature histories from boreholes are well developed [e.g., *Lachenbruch and Marshall*, 1986; *Shen and Beck*, 1991; *Beltrami and Mareschal*, 1991, 1992]. However, the temporal resolution of borehole-based reconstructions is coarse, and can provide only century-to-century estimates of surface and near-surface temperatures. It is difficult to provide shorter-scale temperature variations, i.e., interannual to decadal variability, based on borehole observations. In addition, there are few deep boreholes over the permafrost regions of Russia, and they are not located in diverse landscape and ecosystem settings (e.g., see the map presented in Figure 1 of *Pollack and Smerdon* [2004]). Hence borehole measurements are not ideal for adequately assessing ST fluctuations for different regions of Russia.

[7] However, Russia has an extensive network of meteorological stations (Figure 1) with long-term measurements of both air and soil temperature, and this region is therefore particularly suited for investigating the complex interactions between soil and surface air temperature variability. Recent work attempted to estimate the different responses of ST to SAT changes for various regions underlain by permanently and seasonally frozen soils in Russia [*Chudinova et al.*, 2003]. While these findings generally agree with existing estimates of soil and air warming [e.g., *Vasiliev*, 1999; *Izrael et al.*, 2002], it was shown that the use of linear least squares trends is sometimes inappropriate. For some locations, linear trends, even if high and statistically significant, are misleading and arise due to leverage points (i.e., isolated low/high values at the beginning and/or end of the time series), while the time series themselves do not exhibit any long-term increases/decreases.

[8] Estimating long-term trends in any meteorological parameter requires an understanding of the timescales of its underlying patterns of variability. Unfortunately, ST time series are relatively short (<50 years) for the proper detection of long-term temperature variations. However, relatively long SAT time series are available from various sources. If

a relationship can be established between short- and long-term changes in SAT and ST for a region, it would enable the prediction and reconstruction of ST changes based on SAT.

[9] The goal of this work is to determine the oscillatory and trend components in the time series of SAT and ST for various regions in Russia, and to understand the response of ST to changes in SAT. We employ Singular Spectrum Analysis (SSA) to determine the trends and oscillations in SAT and ST time series. This investigation focuses on the permafrost regions of Russia which occupy approximately 60% of the area and are located mostly in its Asian territory [*Yershov*, 1998]. We focus on five regions (Figure 1) defined in our previous work [*Chudinova et al.*, 2003]: (1) West Siberian Plain (18 stations), (2) western Central Siberian Plateau (45 stations), (3) eastern Central Siberian Plateau (28 stations), (4) Transbaikalia (27 stations), and (5) the territory to the east of the Lena River (15 stations). These regions correspond to established soil/geographical zones (e.g., the northern boundary of the region corresponds to the southern boundary of tundra soils) and geographical regions of Russia.

2. Data and Methods

[10] We use mean monthly ST data (obtained by extraction thermometers with an accuracy of 0.1°C) from meteorological stations in Russia. The data were obtained from the Frozen Ground Data Center (http://nsidc.org/fgdc/) at the National Snow and Ice Data Center (http://nsidc.org/), University of Colorado at Boulder. Detailed descriptions of the ST measurements are provided by *Gilichinsky et al.* [1998] and *Zhang et al.* [2001], and this data set has been used successfully to characterize numerous aspects of frozen ground variability in Russia [e.g., *Frauenfeld et al.*, 2004; *Zhang et al.*, 2005]. If available for the same locations, mean monthly SAT data were obtained from the All-Russian Research Institute of Hydrometeorological Information-World Data Center (RIHMI-WDC; http://www.meteo.ru/data/emdata.htm) [*Vose et al.*, 1992]. As air temperatures are unavailable for most stations, or the available SAT record is too short (20–30 years), a majority of the SAT data are substituted from the *New et al.* [2000] data set of global monthly air temperatures, available on a $0.5^\circ \times 0.5^\circ$ grid for 1901–1995. The proportion of substituted data represents 86, 66, 90, 75, and 100% for regions I–V, respectively. Data were extracted for the grid cell center closest to a station.

[11] Most of the available ST time series are relatively short (25–40 years) and have gaps due to missing data. Thus analysis of both long- and short-term trends and oscillations is not possible for all individual stations. We therefore analyze regionally averaged ST time series, similar to *Hu and Feng* [2003] and *Frauenfeld et al.* [2004]. However, the five regions were selected based on their similar underlying patterns of SAT and ST variability [see *Chudinova et al.*, 2003], and our spatial averaging is therefore performed only for uniformly varying regions. Composite time series are created for each of the five regions based on the stations' departures from a long-term mean: 1969–1990 for ST and 1960–1990 for SAT. These base periods were necessitated by data availability; rather than use the same, but shorter 1969–1990 period in our calculation of SAT departures, we decided to employ the more widely used 30-year base period to allow for better comparisons with the existing literature. Furthermore, the 1969–1990 versus 1960–1990 base periods yielded very similar SAT departures (not shown). Composite time series were also generated for mean annual and seasonal ST (for 1960–1990) and SAT (for 1902–1995) departures. Seasonal averages are created for winter (December–February), spring (March–May), summer (June–August), and autumn (September–November). Annual ST time series are analyzed at depths of 0.4 m, 1.6 m, and 3.2 m, and seasonal ST time series for 0.4 m. Finally, all composite time series were standardized with respect to their mean and standard deviation to allow for appropriate comparisons.

[12] SSA serves as the primary methodology and is particularly suitable for this type of research, especially for the treatment of relatively short time series. Furthermore, SSA has proven useful in decomposing time series into their trend and oscillatory components and noise, and has been widely used in the natural sciences: the analysis of paleoclimatic time series [*Vautard and Ghil*, 1989; *Yiou et al.*, 1994, 1995], and climate variability at interdecadal [*Ghil and Vautard*, 1991; *Allen and Smith*, 1994; *Plaut et al.*, 1995; *Robertson and Mechoso*, 1998; *Frauenfeld et al.*, 2005], interannual [*Rasmusson et al.*, 1990; *Castagnoli et al.*, 1999], and interseasonal [*Jevrejeve and Moore*, 2001; *Bardin*, 2002] timescales.

[13] SSA is a nonparametric method whereby the decomposition of a given time series is achieved by utilizing the actual data, instead of by fitting a modeled process. It extracts additive principal components (PCs) without any prior assumption of the time series' underlying structure, and assesses the contribution of each PC to the total variance. SSA entails the following steps.

[14] 1. The first step is an embedding procedure which constructs a sequence of vectors $x(i)$, $i = 1, \ldots, K$ from the original time series $\{Y(i)\}$, $i = 1, \ldots, N$. $K = N - M + 1$, where M is the embedding dimension, or the length of the (embedding) window. This sequence is usually referred to as the $\mathbf{M} \times \mathbf{K}$ covariance (trajectory) matrix.

[15] 2. The second step is an orthogonal decomposition of the trajectory matrix, which provides a number of PCs. Part of the PCs are associated with trend and oscillatory components, and the other part with noise. A pair of PCs in quadrature suggests periodic variability, while a single PC suggests trend.

[16] 3. The final step entails grouping the leading PCs that explain most of total variance, and reconstructing trends as well as oscillatory components.

[17] For a detailed description of this method and further references, see *Ghil et al.* [2002].

[18] In applying SSA, we employed two versions: the "basic" version, which uses the Hankel form ($\mathbf{M} \times \mathbf{K}$) of the trajectory matrix [*Goljandina et al.*, 2001], and the "Monte Carlo SSA" (MC-SSA) version, which uses the Toeplitz form ($\mathbf{M} \times \mathbf{M}$) [*Allen and Smith*, 1994, 1996]. Both versions are used because this work represents a first attempt at applying SSA to short ST time series. Furthermore, the differences between the matrix forms provide a different separation of components for the time series under investigation. According to *Elsner and Tsonis* [1996] and *Gojandina et al.* [2001], the basic version can be successfully applied to nonstationary time series and is more

Table 1. Trend and Oscillatory Components of Annual Air Temperature Time Series, Their Respective Explained Variance, and Associated Principal Components (PCs)[a]

	Basic Method			MC-SSA			MTM	
Region	Oscillation, years	Variance, %	PCs	Oscillation, years	Variance, %	PCs	Red Noise	White Noise
I	trend	9.6	1	**trend (62.5)**	6.8	1	6.4	**trend (35)**
I	6.9	14.3	5,6	6.5	9.2	5,6	**2.7**	**6.8**
I	2.7	16.5	2,3	**2.7**	10.5	2,3	**2**	**2.6**
I	4.7	10.7	8,9					**2.0**
II	trend	13.6	1,2	**trend (55)**	13.6	1,2	**2.6**	trend
II	2.7	9.2	3,4					
II	4.7	8	5,6					
III	trend	16.5	1,2	**trend (62.5)**	**12.5**	**1,2**	**trend (52)**	**trend (52)**
III	4.7	10.9	5,6	4.7	7.6	7,8	4.9	4.9
III	2.7	11.9	3,4	**2.7**	**10.1**	**3,4**	**2.6**	**2.6**
III	2	9	7,8	2.0	8.5	5,6	2.0	2.0
IV	trend	13.9	3,4	**trend (67)**	16.9	1,2	trend	**trend**
IV	5.9	9,7	5,6	6.3	7.0	5,6	4.8	**4.8**
IV	4.8	15,9	1,2	**4.7**	8.9	3,4		
IV	2.6	7.5	7,8					
V	trend	24.8	1,2	**trend (64)**	27.8	1,2	**trend (36)**	**trend (36)**
V	8.7	7.5	5,6	**8.9**	7.7	3,4	**2.8**	**2.8**
V	2.9	9.7	3,4	**2.9**	6.9	5,6		

[a]In Tables 1–4, for MC-SSA and MTM, values in bold are statistically significant at 0.05 level; values in italics are not statistically significant, but they are well separated. The remaining values are statistically significant at 0.10 level. Regions I, II, III, IV, and V designate the West Siberia Plain, western Central Siberian Plateau, eastern Central Siberian Plateau, Transbaikalia, and the territory east of the Lena River, respectively.

suitable for revealing trend components in real (observational) time series. However, a disadvantage of this version and its corresponding toolkit (http://www.gistatgroup.com) is that it does not provide any estimation of the statistical significance of the components detected.

[19] The MC-SSA version uses a Monte Carlo procedure which allows for the testing of individual components against a null hypothesis of red or white noise. In addition, the corresponding SSA-MTM toolkit (http://www.atmos.ucla.edu/tcd/ssa/) includes spectral methods of estimating periodic components such as the multitaper method (MTM), which are suited for detecting periods in relatively short time series. A detailed description of MC-SSA and MTM, as well as the validity of these methods for revealing periodic components in temperature time series, is provided by *Ghil et al.* [2002]. We applied MTM and tested our detected components by this method against null hypotheses of both red and white noise.

[20] First, both methods were applied to the SAT and ST series in order to test their validity for the analysis of nonstationary time series. This reveals all long-term (i.e., trend) components. Next, stationary time series are created by subtracting the mean and the linear trends, and then dividing each series with respect to its standard deviation. Both SSA versions are again applied to the standardized stationary time series for a better detection of periodic components.

[21] We used a maximum embedding dimension (i.e., the window length, M) equal to 45 for SAT, and 15 for ST in order to capture the nonlinear trend with long-term oscillatory components. This proved to be the optimal choice of M, and its robustness is verified by changing the embedding dimension in steps of 5, for SAT in the interval $15 < M < 45$, and for ST in the interval $10 < M < 15$.

3. Results and Discussion

[22] For the specific reconstructed trend and oscillatory components of the SAT and GT time series, their respective explained variance (%), and associated principal components (PCs) please refer to Tables 1–4.

3.1. Validity of Methods Used for Detecting Trends and Periodic Components

[23] The trend components detected based on the nonstationary annual and seasonal SAT time series are found to be nonlinear: they contain both long-term trends (corresponding to a rise in SAT between 1902 and 1995) and oscillatory components. The SSA methodology was able to produce nearly linear components only in some cases. In addition, subtracting the least squares linear trend improved the separability of the components. This was primarily important for the SAT time series, where the proportion of noise is higher than in ST time series. Therefore, in this work, we analyze standardized stationary SAT time series and standardized nonstationary ST time series. For the ST time series, we subtracted the least squares linear trend only when SSA was not able to detect oscillatory components in the original ST time series. In most cases, $M = 45$ was best suited for detecting both trend and oscillatory components in the SAT time series, and M generally ranged from 35 to 45. The best separability of components in the ST time series was achieved at $M = 15$.

[24] Generally, both basic and MC-SSA versions, as well as MTM, detected the same oscillatory components in the SAT and ST time series (see Tables 1–4), suggesting a robustness of our results. The differences in the detected periods arising from differences in method are very small and range from 0.1–0.5 years. Some slight variations in shape are observed as well. However, since the differences are small and the components are coincident with each other, we consider them to be the same components. The variations likely arise from the different computational/mathematical bases of these methods; however, some of the differences could also be attributed to the short length of some of the time series.

[25] Practically all oscillatory components in the SAT time series are statistically significant at $\alpha < 0.10$ according

Table 2. Trend and Oscillatory Components of the Annual Soil Temperature Time Series and Their Respective Explained Variance

		Basic Method			MC-SSA			MTM	
Region	Depth, m	Oscillation, years	Variance, %	PCs	Oscillation, years	Variance, %	PCs	Red Noise	White Noise
I	0.4	trend	24.5	1	**trend**	46.5	1,2	**2.7**	**trend**
I	0.4	7.7	37	2,3	8.9	25.4	3,4		**15.4**
I	0.4								9.5
I	1.6	trend	28.0	1	trend	51.2	1,2	2.7	**trend**
I	1.6	7.7	29.3	2,3	*8.2*	29.5	3,4		
I	3.20	trend	13.7	3	**trend**	23	1	5.7	**9.4**
I	3.20	7.7	49.2	1,2	8.5	35.9	2,3	2.7	
II	0.4	trend	20	1	trend (27)	18.7	1	**2.5**	**13**
II	0.4	**2.7**	34	2,3	trend (12.7)	12.5	4		
II	0.4	trend	12.5	4	trend (9.1)	12.3	5		
II	0.4	7.7	20	5,6	2.6	30.1	2,3		
II	1.60	trend	20	1	**trend**	35.7	1,2	**2.7**	**trend**
II	1.60	2.7	32	2,3	*7.7*	20.4	5,6		
II	1.60	trend	14.7	4	2.7	29.5	3,4		
II	1.60	7.7	17.1	5,6					
II	3.20	trend	66.3	1,2	trend	65.6	1,2	**2.7**	trend
II	3.20				*7.7*	15.0	3,4		
III	0.4	trend	26.6	1	**trend**	37.7	1,2	trend	**trend**
III	0.4	4.3	29.1	2,3	*4.6*	18.0	3,4	**3.0**	
III	1.6	trend	35.7	1	**trend**	49	1,2	trend	**trend**
III	1.6	4.3	21.9	2,3	*4.7*	12.8	3,4	**2.7**	
III	3.2	trend	53.0	1	trend	68.0	1,2	5.2	**trend**
III	3.2	4.3	19.0	2,3	*4.7*	10.3	3,4	**2.7**	
IV	0.4	trend	24.0	1	**trend**	37.5	1,2	**2.4**	**trend**
IV	0.4	2.6	34.4	2,3	2.4	20.1	3,4		
IV	1.6	trend	41.1	1,2	trend	48.3	1,2	**2.5**	**trend**
IV	1.6	2.6	21.8	3,4	*2.6*	14.7	3.4		
IV	3.2	trend	66.1	1,2	trend	61.7	1,2	trend	**trend**
IV	3.2	2.6	13.2	3,4				**2.8**	
V	0.4	trend	19.9	1	trend	47.4	1,2	trend	**trend**
V	0.4	5.4	28.4	3,4	5.8	18.3	3,4	**4.5**	4.5
V	1.60	trend	15.0	2	**trend**	20.3	1	**trend**	**trend**
V	1.60	trend (5.6)	13.5	3	**5.8**	27.1	2,3	**4.5**	**4.6**
V	1.60	trend (2.0)	20.7	1				**2.0**	2.0

to the Monte Carlo method and MTM. The reliability of oscillatory components detected in seasonal SAT time series is higher: three quarters of them are statistically significant at $\alpha < 0.05$. Using MTM, practically all oscillatory components have the same significance level against both red and white noise background.

[26] For the ST time series, MC-SSA and MTM confirmed the reliability ($\alpha < 0.05$) of the oscillatory components with a period $\leq$5 years. The lower-frequency components with periods from 6 to 9 years in the ST time series are not statistically significant ($\alpha < 0.05$). Nevertheless, these components are easily detectable, associate with two PCs (in quadrature), and explain up to 30% of the total variance. Therefore we believe these 6 to 9 year oscillatory components to nonetheless be physically meaningful. It appears that the ST time series may simply be too short for proper component detection.

[27] Practically all of the long-term components detected in both SAT and ST time series have a nonlinear form. Therefore there are two kinds of components. First, there are low-frequency components with period lengths from 30 to 60 years. They are associated with a pair of PCs in quadrature, and are hence technically considered to be oscillatory components. However, due to the lengths of the SAT time series investigated only one to two periods of these ''oscillations'' can be observed, which does not justify classifying them as oscillatory components. On the other hand, it is possible for trends to have the shape of an oscillation, but they are reconstructed on the basis of only one PC (e.g., the ST time series for region II). Second, there are trends having the shape of an oscillation, (e.g., the ST time series for region II). We will consider all such components as trends, but will nonetheless note their period.

[28] In contrast to SAT, the reliability of trend components in ST time series against the null hypothesis of white noise (in MTM) is higher than against red noise. It seems white noise may be a more appropriate background for ST than red noise, perhaps due to the attenuation of high-frequency fluctuations of temperature with depth.

[29] The shapes of the trend components detected by both SSA methods and MTM differs in both SAT and ST time series, even for stationary time series. As seen from Figure 2d, the basic version is more sensitive to changes in temperature: the long-term trend reconstructed using the basic version is able to account for the sharp rise in annual SAT beginning in 1980 over western Central Siberia and Transbaikalia, whereas the MC-SSA version is not. Therefore we analyze both the trend and periodic components reconstructed with the basic version and use MC-SSA and MTM to estimate the statistical significance of the components we detect.

3.2. Comparisons of Components in the Annual SAT and ST Time Series

[30] The nonlinear components reconstructed in annual SAT time series (Figure 2) show that the current rise in SAT across each of the five study regions could be the ascending part of a new long-term oscillation. These components are significant at the 0.05 α level. The most recent increase in

Table 3. Trend and Oscillatory Components of the Seasonal Air Temperature Time Series and Their Respective Explained Variance

	Basic Method			MC-SSA			MTM	
Region	Oscillation, years	Variance, %	PCs	Oscillation, years	Variance, %	PCs	Red Noise	White Noise
				Winter				
I	9.8	16.3	1,2	**9.7**	12.7	1,2	**10**	**9.9**
I	2.7	13.4	3,4	**2.6**	9.5	3,4	**2.6**	**2.6**
I				2.7				
II	9.8	13.5	1,2	**9.8**	14	1,2	**9.9**	**9.9**
II	2.9	10.7	5,6	2.7	9.9	3,4	2.8	2.8
II	2.3	12.1	3,4	2.3	8.5	5,6	2.3	2.3
III	trend (60)	5.4	5	**trend (62)**		1,2	**trend(48.8)**	**trend (48.8)**
III	4.7	14.9	1,2	**4.7**		3,4	4.6	4.6
III	2.7	12.9	3,4	**2.7**		5,6	2.8	2.8
IV	8.0	11.2	4,5	*trend*	5.3	1	trend (40)	trend (40)
IV	4.8	10.3	6,7	**10.5**	9.0	4,5	2.0	
IV	2.7	12.3	2,3	4.8	8.2	6,7		
IV				**2.7**	9.5	2,3		
V	2.3	12.0	3,4	**20.5**	10.8	3,4	**3.1**	27.7
V	2.1	15.8	1,2	3.0	9.8	5,6	**2.2**	**3.1**
V				**2.3**	13.6	1,2		**2.2**
				Spring				
I	5.7	17.1	1,2	**5.6**	10.0	3,4	**2.8**	**2.9**
I	3	13.1	3,4	**2.9**	11.0	1,2		
I								
II	24	13.2	1,2	**23.5**	10.1	1,2	**32**	**32**
II	4.7	10.1	6,7	**4.7**	7.2	5,6	4.4	4.4
II	2.7	11.1	4,5	**2.8**	9.1	3,4	2.9	2.9
II							2	2
III	trend (45)	6.4	3	**trend(47.6)**	8.8	5,6	8.1	32
III	4.7	13.1	4,5	7.6	12.9	1,2	4.8	8.1
III				**4.7**	9.1	**3,4**	2.2	4.9
IV	22	13.2	3,4	*22*	12.7	3,4	7.0	**trend (33)**
IV	4.7	22.7	1,2	**7.0**	10.4	5,6	**4.8**	**7.0**
IV				**4.7**	16.0	1,2	**3.5**	**4.8**
IV								3.5
V	4.5	15.5	1,2	**4.7**	11.3	1,2	**4.8**	**4.8**
V	3.0	13.3	3,4	**2.7**	9.5	3,4	2.8	2.8
				Summer				
I	trend (33)	16.6	1,2	**trend (33)**	15.0	1,2	7.5	**trend (53)**
I	7.5	12.4	3,4	**7.5**	8.3	5,6	2.8	**7.5**
I				**2.4**	8.5	3,4	**2.4**	2.0
II	11.7	11.1	5,6	**trend (12.3)**	5.2	4	**14.4**	**14.4**
II	5.4	13.2	3,4	**5.4**	10.5	1,2	**5.8**	**5.8**
II	2.0	16.1	1,2				**2.2**	**2.2**
III	19.2	14.5	1,2	**20**	10.4	3,4	**24**	**24**
III	6.7	8.1	7,8	3.5	11.3	1,2	**3.7**	**3.7**
III	3.5	11.9	3,4	**2.0**	8.4	5,6	**2.5**	**2.5**
III	2.5	8.9	5,6				**2.2**	
IV	33	7.7	7,8	**trend (47)**	9.1	5,6	trend (37)	trend (37)
IV	7	6.5	9,10	**5.1**	10.8	3,4	**5.4**	**5.4**
IV	5.2	12.4	3,4	**2.2**	18.2	1,2	2.1	2.1
IV	2.3	19.2	1,2	**2.1**	7.2	7,8		
IV	2.1	10.4	5,6					
V	trend	26.1	1,2	**trend (55.8)**	22.7	1,2	trend	**trend**
V	20.5	12.7	3,4	**19.6**	12.8	3.4	6.8	**6.8**
V				**7.4**	5.1	5,6	4.3	
V				4.3	6.7	7,8		
				Autumn				
I	trend (60)	8.6	1	9.2	15.4	4,5	**trend (34)**	**trend (36)**
I	6.4	10.3	4,5	**3.9**	18.1	2,3	**3.9**	**9.1**
I	3.9	15.7	2,3	**2.0**	9.8	1	**2.5**	**4.0**
II	trend (60)	12.8	5,6	*trend*	6.4	3	trend (33.6)	trend (33.6)
II	2.5	15.4	1,2	**2.6**	14.9	1,2	**2.6**	**2.6**
II	2.0	13.3	3,4	**2.2**	9.8	4,5	**2.2**	**2.2**
III	5.7	9.3	6,7	5.7	8.6	6.7	**2.7**	**2.7**
III	2.9	10.5	4,5	**2.7**	10.0	4,5	**2.0**	**2.0**
III	2.5	16.8	2,3	**2.5**	17.2	1,2		
III	2	11.3	1					
IV	trend (60)	13.2	3,4	**trend (60)**	12.8	2,3	**2.4**	**2.4**
IV	5.8	12.0	5,6	**5.7**	8.5	6,7	**2.1**	**2.1**
IV	2.1	15.2	1,2	**2.1**	9.8	4,5		

Table 3. (continued)

	Basic Method			MC-SSA			MTM	
Region	Oscillation, years	Variance, %	PCs	Oscillation, years	Variance, %	PCs	Red Noise	White Noise
V	trend (60)	27.5	1,2	**trend (65)**	26.1	1,2	**trend (33)**	**trend (33)**
V	3	10.0	5,6	3.3	10.6	3,4	**3.3**	**3.3**
V	2	12.2	3,4	2.0	6.1	5,6	**2.0**	**2.0**

air temperature exceeds the warming of the preceding period over the Central Siberian Plateau and Transbaikalia (Figures 2b, 2c, and 2d). In addition, least squares linear trends extracted from the annual SAT time series in these regions show a significant (0.05 level) increase in SAT for the period 1902–1995: 0.15 and 0.09°C/10 yr for the western and eastern Central Siberian Plateau, respectively, and 0.14°C/10 yr for Transbaikalia. The recent warming in region V (east of the Lena River) is very similar to the warming of the preceding period (Figure 2e). These results generally agree with estimates of SAT changes in Russia made by *Serreze et al.* [2000] on the basis of linear trends,

Table 4. Trend and Oscillatory Components of the Seasonal Soil Temperature Time Series at 40 cm and Their Respective Explained Variance

	Basic Method			MC-SSA			MTM	
Region	Oscillation, years	Variance, %	PCs	Oscillation, years	Variance, %	PCs	Red Noise	White Noise
				Winter				
I	trend	55	1,2	**trend**	58	1,2	-	**trend**
I				2.7	17	3,4		
II	8.6	24.9	3,4	9.0	22.0	3,4	**2.6**	**2.6**
II	2.7	39	1,2	**2.7**	38.1	1.2		
III	trend	18.3	1	**trend**	17.8	1		**trend**
III	4.3	28.2	2,3	4.4	21.6	2,3		
IV	trend	18.3	1	**trend**	34.6	1,2	2.4	**trend**
IV	2.6	31.5	2,3	2.6	23.8	3,4		
V	trend		3	**trend**	24	1	trend	**trend**
V	5.4	26.8	4,5	5.6	25.3	2,3	**2.0**	**2.0**
V	2.1	38.2	1,2	2.1	20.6	4,5	-	-
				Spring				
I	trend	47.1	1,2,3	**trend**	33,4	1,2	**2.8**	**trend**
I	6.6	33	1,2	trend	11.2	3	-	-
II	trend	12	3	*trend*	13.0	1	-	-
II	2.7	34	1,2	**2.6**	21.9	3,4	3.0	3.0
III	trend	22.8	1	**trend**	26.5	1	trend	**trend**
III	4.3	28.5	2,3	-	-	-	-	-
IV	2.6	29.6	1,2	-	-	-	-	-
IV	-	-	-	-	-	-	-	-
V	-	-	-	trend	10.6	3	**4.6**	trend
V	-	-	-	5.0	13.5	1	**2.1**	**4.6**
				Summer				
I	trend	11	3	trend	13	3	**2.8**	**8.5**
I	8.7	34	1,2	**8.5**	34.3	1,2		6.5
II	trend (12.0)	29	1,2	**trend (13.3)**	26.4	1,2	**2.4**	**trend (14.8)**
II	5.4	23.1	3,4	**5.2**	18.2	3,4		
III	6.4	25.6	2,3	trend	15.7	1	trend	**trend**
III	trend	10.0	5	trend	13.1	2	**2.0**	**2.0**
III	-	-		trend (6.6)	8.6	5		
III	-	-		2.0	22.8	3,4		
IV	10.0	10.4	4,5	**trend (12.9)**	16.4	1	5.4	5.4
IV	5.8	31.4	2,3	*trend* (5.4)	14.0	2	**2.0**	**2.0**
IV	2.1	18	1	2.1	25.3	3,4		
V	3.2	35.6	1,2	trend	15.6	1	**3.4**	trend
V				3.2	26.4	2,3		
				Autumn				
I	trend	23	4,5	trend	18	1	**trend**	**trend**
I	3.8	31.8	2,3	**3.9**	32.6	2,3	3.7	3.7
II	7.4	21.8	3,5	7.3	18.3	3,4	**2.0**	**2.0**
II	2.0	31.8	1,2	**2.0**	26.4	1,2		
III	4.6	29.0	3,4	*4.7*	21.8	3,4	**2.3**	2.7
III	2.5	43.6	1,2	**2.5**	37.2	1,2		**2.3**
IV	trend (10.0)	22.2	3,4	*trend (11.0)*	20.9	3,4	**2.0**	**2.0**
IV	2.1	34.5	1,2	**2.0**	34.5	1,2		
V	trend	12.9	3	trend	30.5	1	trend	**trend**
V	4.0	41.5	1,2	**3.9**	29.2	2,3	**4.5**	**4.5**

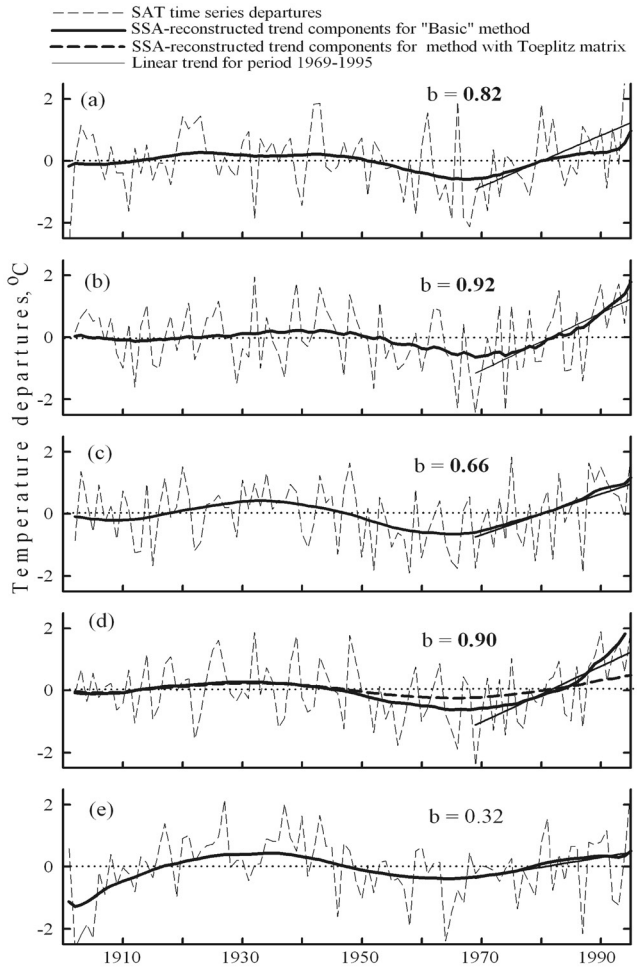

Figure 2. Stationary annual SAT time series departures and SSA-reconstructed long-term trend components for the five regions; "b" refers to the regression trend, in °C/10 yr. Significant coefficients (0.05 level) are bold. (a) West Siberia Plain, (b) west part of Central Siberian Plateau, (c) east part of Central Siberian Plateau, (d) Transbaikalia, and (e) territory to the east of Lena River.

except for the West Siberian Plain where the SSA-reconstructed trend shows little increase in annual SAT. This may be due to the fact that the least squares linear method overestimates trends for relatively short time series, in comparison with the SSA-reconstructed trend (e.g., Figure 2a).

[31] The trend components in the ST time series vary in shape and slope (Figure 3). A gradual increase in ST in the period 1960–1990 is typical only for the eastern Central Siberian Plateau and the territory located to the east of the Lena River (Figures 3c and 3e). In the other regions, we observe a period of cooling from the mid-1960s to the mid-1970s, followed by an increase in annual ST at all depths, except for West Siberia.

[32] For West Siberia, the western Central Siberian Plateau, and Transbaikalia, a coincidence in minima is observed in the trend components of SAT and ST for the depth of 0.4 m, as well as a shift in minima for ST with depth (Figures 3b and 3d). It is likely that the trend components detected in these ST time series are part of a period's long-term oscillatory component, corresponding to a phase shift between an oscillatory component in SAT of period ~60–70 years, which was also identified by *Marcus et al.* [1999], and a corresponding component in ST. As seen from Figure 3, the amplitude of the oscillation increases with depth. There could be two explanations for this: first, the standardization of the time series essentially removes much of the attenuation with depth; second, we did not conduct any prefiltering of the time series and hence the results of the SSA are dependent on the ratio between the components and noise. The proportion of trend-explained variance increases with depth due to the attenuation of high-frequency fluctuations. As a result, the amplitude of the oscillation (nonlinear trend) increases.

[33] A phase shift in ST with depth is not observed for the eastern part of the Central Siberian Plateau or the territory to the east of the Lena River (Figures 3c and 3e). This could be due to the fact that cooling in these regions occurs in the early to mid-1960s (Figures 2c and 2e), and that the length of these ST time series is not sufficient to clearly detect minima in the ST time series.

[34] An oscillatory component with periods of 2–2.7 years is generally observed in the annual SAT over all five regions, and accounts from 6.7 to 16.5% of the total variance. An oscillation with a period around 4.7 years accounts for 10–15% of the variance in the annual SAT time series over the Central Siberian Plateau (western and eastern parts) and Transbaikalia. A 6.9 year oscillatory component predominates in annual SAT of the West Siberia

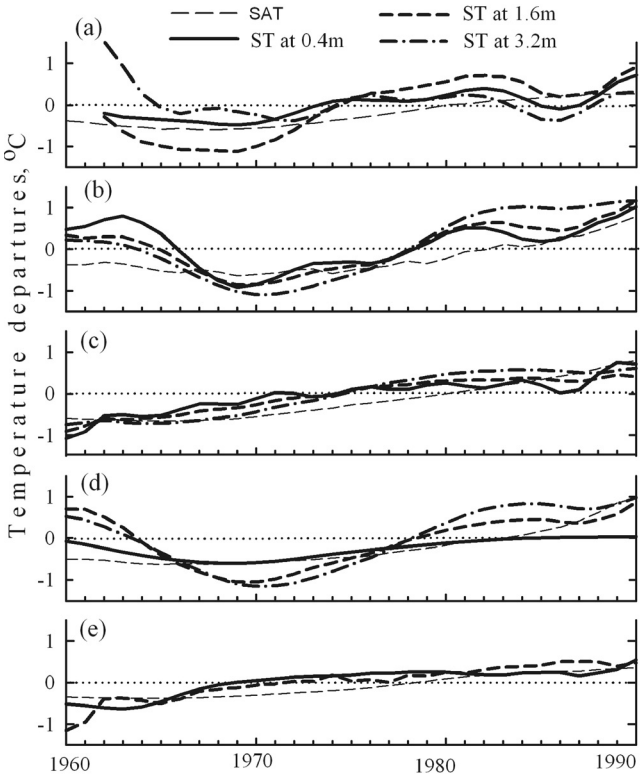

Figure 3. SSA-reconstructed long-term components in annual SAT and ST departures at 0.40 m, 1.6 m, and 3.2 cm. (a–e) As in Figures 2a–2e.

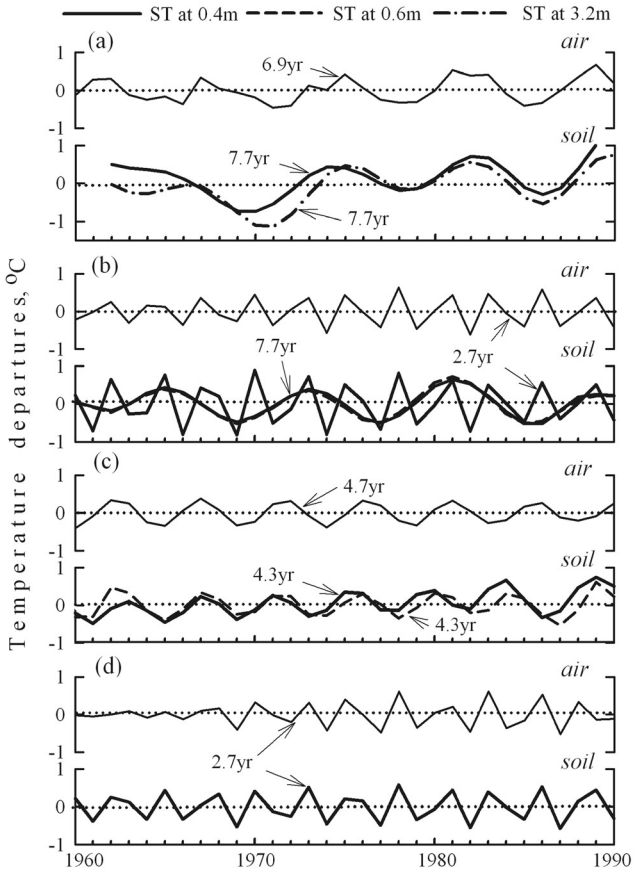

Figure 4. SSA-reconstructed oscillatory components in annual SAT and ST temperature time series departures. (a–d) As in Figures 2a–2d. Note that there is no Figure 4e because no oscillatory components were detected in the territory east of the Lena River.

Plain, and an 8.9 year oscillation is observed in annual SAT east of the Lena River.

[35] Figure 4 shows the oscillatory components reconstructed in annual ST time series and the corresponding oscillations in annual SAT. An oscillation with the longest period (7.7 years) was detected in ST time series of West Siberia (Figure 4a), and the oscillatory components (period 6.9 years) between 1960 and 1990 in the corresponding SAT time series have closely related phases between 1960 and 1990. The observed small differences in the average period of the annual SAT and ST components could again be due to the fact that the ST time series is too short to precisely calculate the oscillation's period. SSA detected a 4.3 year oscillation in the annual ST time series of the eastern Central Siberian Plateau (Figure 4c). This oscillatory component is close to the 4.7 year component in the corresponding annual SAT time series but their phases are not perfectly coincident for period 1960–1990 (Figure 4c). Oscillations with a period of 2.6–2.7 years dominate the annual ST time series in the western Central Siberian Plateau and in Transbaikalia (Figures 4b and 4d). They are coincident with the 2.7 year oscillatory components in the corresponding SAT time series over these regions (Figure 4). A 7.7 year oscillation is detected in the annual ST time series at 0.4 m and 1.6 m (Figure 4b) in the western Central Siberian Plateau but it does not correspond to any oscillations in the SAT time series. No oscillatory components with similar length of period were detected in the annual SAT and ST time series for the territory east of the Lena River.

[36] According to a one-dimensional conductive framework, a temperature wave should attenuate as it penetrates the ground, with an analogous phase shift. As seen from Figures 3 and 4, the behavior of some components reconstructed in the ST time series may be contradictory to such a framework. The amplitude of many oscillatory components and nonlinear trends are either the same, or some increase with depth. However, e.g., Figure 4 does illustrate a clearly detectable phase shift (~1 year) from 0.4 m to 3.2 m for the 4.3 year oscillation after 1970 for the eastern Central Siberian Plateau (Figure 4c). A shift close to two years exists between ST minima, detected between the 0.4 m and 3.2 m depths in Western Siberia. No phase shift is evident for the other oscillatory components. This could be partly due to the temporal scale employed here; interannual fluctuation of SAT and ST are analyzed, therefore only phase shifts equal to year and longer can be detected. However, as these phase shifts are an important consideration in the SAT-ST coupling, we will revisit this issue in section 4.

3.3. Comparisons of Components in the Seasonal SAT and ST Time Series

3.3.1. West Siberian Plain

[37] We found that an increase in SAT in the period from 1960 to 1995 occurred in summer and autumn (Figure 5a). This warming is part of an oscillation with a period of 33 years in summer, and part of a trend with a 60 year period in autumn. No long-term components are found in the winter and spring SAT time series; oscillatory components with periods of 9.8 and 2.7 years dominate in winter, and periods of 5.9 and 3 years dominate in the spring SAT time series. In addition, oscillations of 7.7 and 3.8 years were detected in summer and autumn SAT time series, respectively. Oscillations with similar periods in winter and summer SAT time series for this territory have previously been reconstructed by *Bardin* [2002]. It is interesting that the oscillation of period 7.7 years in the summer SAT time series is coincident with the preferred 7.7 year oscillations of the winter North Atlantic Oscillation (NAO), as reported by *Jevrejeve and Moore* [2001] and *Gamiz-Fortis et al.* [2002]. Generally, a strong correlation is observed between concurrent winter NAO index and winter SAT. However, a similar winter–summer relationship was also reported by *Ogi et al.* [2003a, 2003b]. They found that the high-latitude summer climate in the Northern Hemisphere is influenced by the NAO of the previous winter [*Ogi et al.*, 2003a]. Furthermore, winter NAO has a significant relationship with summer climate during years of solar maximum for several regions of the Northern Hemisphere, in particular Western Siberia [*Ogi et al.*, 2003b].

[38] SSA-reconstructed trend components in the winter, spring, and autumn ST time series show a nonlinear increase in ST starting in the mid 1960s and ending after 1973/1974 (Figure 6a). Only the summer trend shows a persistent rise of ST during period 1960–1990. Of the oscillatory components (Figure 7a), those in the summer

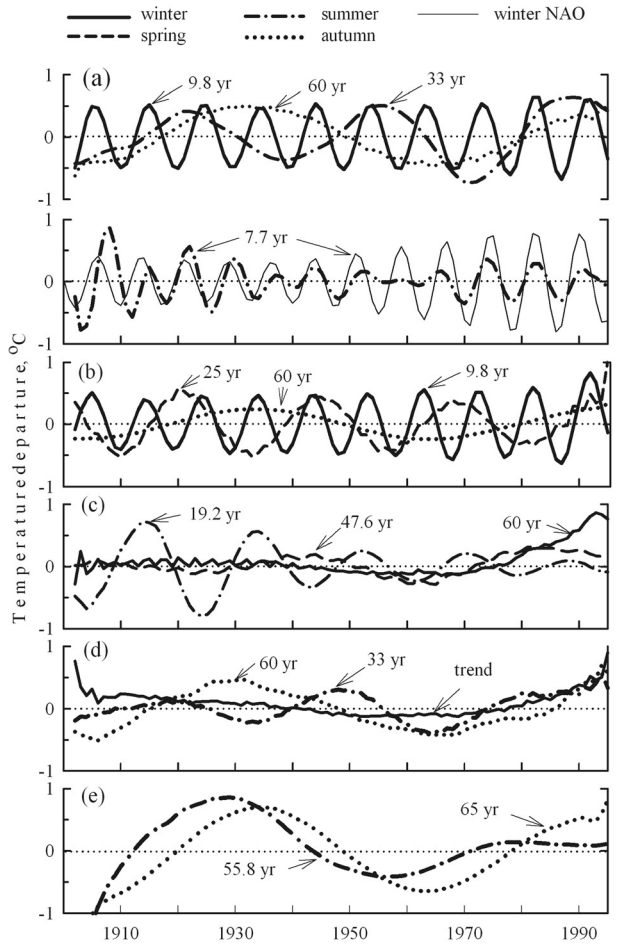

Figure 5. SSA-reconstructed trend and long-term oscillatory components in the seasonal SAT time series. (a–e) As in Figures 2a–2e.

(7.7 year period) and autumn (7.7 year period) ST time series are coincident with the corresponding components in the SAT time series. (We do not consider the 2.7 year component in the winter ST time series, because it is detected by MC-SSA only.) The oscillatory components in summer SAT and ST are different in average period (7.7 versus 8.7 years, see Tables 3 and 4), however they are coincident between 1960 and 1990 (Figure 7a). In addition, these oscillations are coincident with oscillations in annual SAT and ST time series for this region (Figure 4a). Thus we can assume that both short- and long-term changes in summer SAT dominate changes in annual SAT and ST in this region.

3.3.2. Western Central Siberian Plateau

[39] Positive least squares linear trends extracted from the seasonal SAT time series are statistically significant for winter (0.35°C/10 yr), spring (0.13°C/10 yr), and autumn (0.12°C/10 yr). As seen in Figure 5b, the detrended SAT time series' long-term trend (with period ~60 years) detected in the autumn SAT time series exhibits a maximum in the last cycle of the mid-1990s. Like in the West Siberia Plain, an oscillatory component with a period close to 10 years is clearly detectable in the winter SAT time series, and the maximum of its last cycle falls in 1993–1994. In addition, this maximum exceeds maxima of preceding cycles. The maximum of an oscillation with 25 year period in the spring SAT time series also falls in the mid-1990s. Such a coincidence in oscillation maxima is unprecedented in the observational record. This implies that the strong rise in annual SAT observed in the period 1990–1995 (Figure 2b) is driven by this temporal coincidence of maxima of oscillatory components.

[40] A long-term trend was detected in spring ST time series only, but it does not exhibit a rise in ST during the period 1960–1990 (Figure 6b). We were not able to detect any trend in the autumn ST time series using SSA, but the least squares linear trend extracted from this time series was significant at the 0.05 level. It is possible that this linear trend tracks the ST increase in the autumn SAT time series.

[41] Among ST oscillatory components (Figure 7b), only one with a period of 8.6 years in winter and one with a period of 5.4 years in summer are coincident with corresponding oscillations in SAT time series. In addition, the winter component is coincident with oscillations of the 7.7 year period recognized in the annual ST time series (Figure 4b). As in the West Siberian Plain, differences in the averaged periods of these components could be due to the short length of the time series. Although oscillations with periods of 2–3 years were reconstructed in both SAT and ST time series, most of them are not coincident. However, an oscillation with a 2.7 year period in the winter and spring ST time series is coincident with a 2.7 year oscillation in the annual ST time series (Figure 7b).

[42] Summarizing these results, we conclude that detectable annual ST oscillations are driven by ST oscillations during the cold season (winter and spring), although only one of them is dictated by a change in winter SAT.

3.3.3. Eastern Central Siberian Plateau

[43] Air temperature has risen during winter and spring in the eastern Central Siberian Plateau (Figure 5c). This rise is

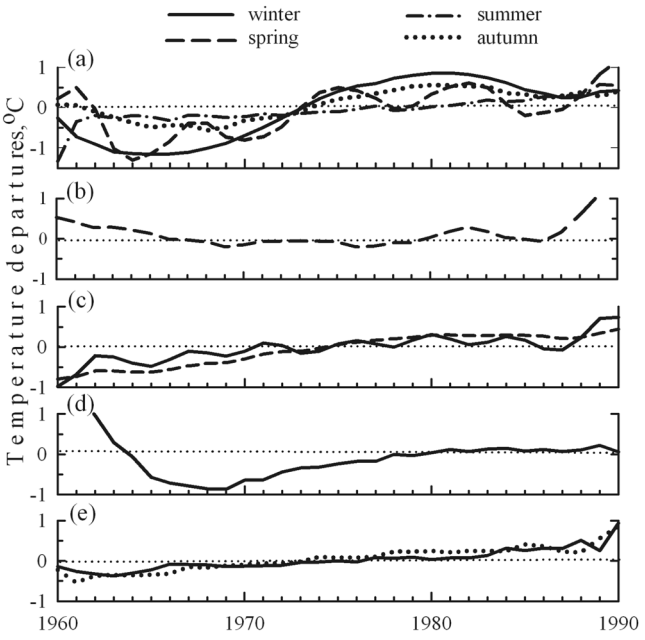

Figure 6. SSA-reconstructed trends in the seasonal ST (at 0.4 m) time series. (a–e) As in Figures 2a–2e.

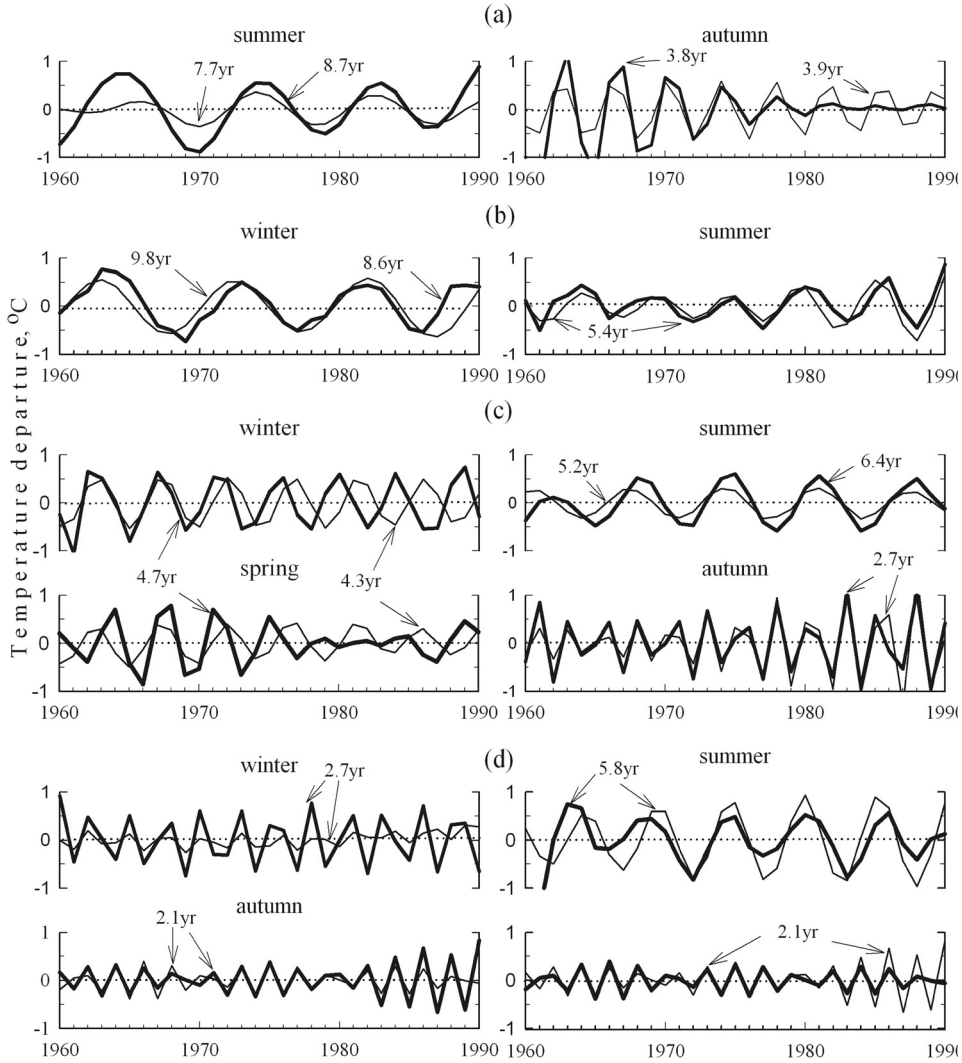

Figure 7. SSA-reconstructed oscillatory components that are in phase in the seasonal ST at 0.4 m (thick line) and SAT (thin line) time series. (a–e) As in Figures 2a–2e.

the ascending limb of a ~62 year period in winter, and a 47–48 year period in spring. The winter component demonstrates an abrupt rise in SAT (approximately 1°C for 1970–1995), which began at the end of the 1960s and exceeds the warming of previous periods. The peak of the last cycle in the spring SAT time series occurs in the mid-1980s, and it is higher than the peaks of the preceding cycles as well.

[44] A long-term oscillatory component (19.2 year period) in summer SAT has a damped sinusoidal shape, and the amplitude of the last period does not exceed 0.2°C. Thus summer warming provides little contribution to the recent annual air temperature increases in the eastern Central Siberian Plateau. The other dominant components in winter and spring SAT are coincident oscillations (Figure 7c) with a period of 4.7 years.

[45] The long-term trends reconstructed in winter and spring ST time series show an increase in ST from 1960 to 1990 (Figure 6c). An oscillation of period 4.3 years in winter and spring ST is coincident with a component of similar period detected in the annual ST time series (Figures 4c and 6c). However, as seen from Figure 4c, this oscillation is not coincident with the shorter-time component (4.7 year period) in the SAT time series. This may also account for the lack of coincidence in the same components for the annual SAT and ST time series (Figure 4c). Only in the summer and autumn time series do we find oscillations that are coincident with ST time series; their periods are 6.7 years in summer and 2.7 years in autumn (Figure 7c).

[46] Thus, although the oscillatory components reconstructed in SAT and ST time series are coincident in summer and autumn, annual ST cycles are controlled by ST dynamics in the upper soil layers in winter; the long-term rise in annual ST is determined by the rise of SAT in winter and spring.

3.3.4. Transbaikalia

[47] Positive least squares linear trends extracted from the initial seasonal SAT time series were statistically significant at the 0.05 level for winter (0.32°C/10 yr), spring (0.11°C/10 yr), and autumn (0.15°C/10 yr). After removal of the

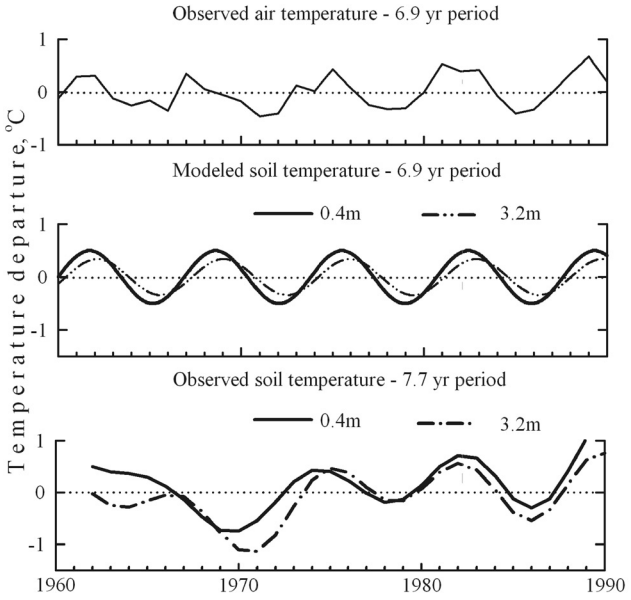

Figure 8. (top) Original SAT time series, (middle) the resulting modeled soil temperatures, and (bottom) for comparison, the corresponding actual/observed soil temperature time series.

least squares linear trend the SSA-reconstructed trends show an increase in SAT beginning around 1960–1965 in winter, summer, and autumn (Figure 5d). There are some potential difficulties in the detection of trend in the winter time series. The basic method was not able to separate any trend and the shape of the trends detected by MC-SSA and MTM are different. MC-SSA indicated a rise in SAT around the mid-1960s (Figure 5d), but this trend is not significant. MTM did detect a significant long-term trend, but this trend does not reflect the strong rise in SAT over the last 30 years of 20th century. This could be due to the observed strong interannual SAT variability during winter.

[48] As seen from Figure 5d, and similar to the western Central Siberian Plateau, the strong rise in annual SAT over the last 30 years of the 20th century is dictated by a coincidence of ascending branches of cycles, albeit with different periods. Additionally, this rise is related to oscillatory components with an average period of 8.0 years in winter SAT. The maximum of its last cycle falls around 1993–1994, as was the case for the western Central Siberian Plateau.

[49] In spite of the rise in SAT beginning around the mid-1960s in practically all seasons, SSA detected a trend component in ST only for the winter time series. This trend reflects a rise in ST only between 1960 and 1980 (Figure 6d).

[50] As seen from Figure 7d, short-term oscillations in summer (2.1 and 5.8 year periods), autumn (2.1 years), and winter (2.7 year period) are coincident with similar oscillations in SAT time series. It seems the autumn and winter components are manifested in the annual ST time series (Figure 4d). Oscillations with periods of 10 and 11 years in summer and autumn ST are detected by both the basic method and MC-SSA. They can probably be explained by other environmental factors, e.g., precipitation and soil moisture, since they are not detected in the corresponding SAT time series. We find no oscillations in the spring ST time series at 0.40 m. Thus the long-term rise in annual ST in Transbaikalia is best explained by the increase in ST during winter and autumn, which is dictated by an increase in SAT in these seasons.

3.3.5. Territory to the East of the Lena River

[51] The trend component (period ~60 years) reconstructed in summer and autumn SAT time series east of the Lena River shows a rise in SAT after the mid-1960s (Figure 5e). As seen from Figure 6e, SSA was able to reconstruct trend components showing an increase in the 0.4 m ST between 1960 and 1995 only for winter and autumn. The winter ST illustrates a short oscillation with a 2.7 year period, which also occurs in the corresponding SAT time series. However, as is the case for the oscillatory components reconstructed in corresponding ST and SAT time series during other seasons, they are not coincident. Thus, as in the western Central Siberian Plateau and in Transbaikalia, the increase in annual ST is driven by soil temperature dynamics in the upper soil layers in winter and autumn.

4. Heat Conduction and Phase Shifts

[52] An important issue when dealing with the response of ST to SAT forcing is the basic physical connection between SAT and ST. In a one-dimensional conductive framework, a temperature wave should attenuate as it penetrates the ground, with an analogous phase shift. To illustrate this heat transfer process, we use the 6.9 year periodicity observed in the annual SAT time series for the West Siberia Plain (Figure 4a) and calculate the corresponding ST regime. For the upper boundary condition:

$$T_g(t) = \overline{T_0} + A_0 \cos(\omega t) \tag{1}$$

we calculate

$$T(x,t) = \overline{T_0} + G_0 x + A_0 e^{-x\sqrt{\omega/2D}} \cos\left(\omega t - x\sqrt{\frac{\omega}{2D}}\right) \tag{2}$$

where T_g is ground surface temperature, or air temperature (°C) in this example; $\overline{T_0}$ is annual mean air temperature (°C); G_0 is temperature gradient (°C m^{-1}); x is soil depth (m); A_0 is amplitude of annual ground surface temperature (°C); $\omega = {}^{2\pi}/_{P}$ and P is period; D is thermal diffusivity (m^2 yr^{-1}); and t is time (years). In this calculation, $\overline{T_0}$ is 0°C due to the removal of the long-term mean in the SAT time series. The term G_0x is ignored due to the shallow depth (up to 3.2 m). We use A_0 = 0.5°C, and D = 31.536 m^2 yr^{-1}. This thermal diffusivity value was selected to generally fit the site characteristics of the data employed. It should be noted that the presented results (below) are sensitive to this selection of thermal diffusivity, however it would not change our main conclusions.

[53] The 6.9 year period in the SAT time series (Figure 8, top) results in a 6.9 year soil temperature periodicity, as evident from Figure 8 (middle). As expected, the temperature wave attenuates with depth, and the analogous phase shift Δt, calculated as

$$\Delta t = x\sqrt{{\pi}/{PD}} \tag{3}$$

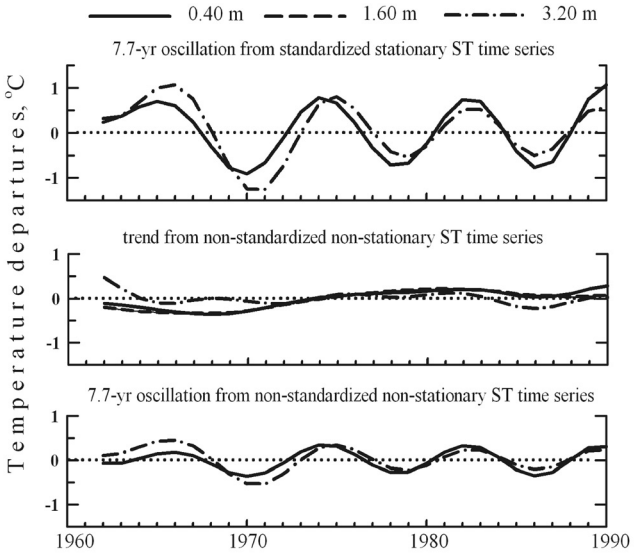

Figure 9. (top) Oscillation from standardized stationary ST time series and (middle) trend and (bottom) oscillation from nonstandardized nonstationary ST time series for West Siberia.

is 0.048 years or 17.5 days at 0.4 m depth, and 0.385 years or 140 days at 3.2 m depth. The corresponding ST components, as can be seen in Figure 8 (bottom), roughly resemble the modeled components with a similar periodicity of 7.7 years, especially after the mid-1970s. However, the modeled attenuation and phase shift are not evident in the actual observations.

[54] There could be a number of reasons for this, such as the nonstationarity of the ST time series. As stated previously, we applied SSA to nonstationary ST time series since we are interested in estimates of long-term changes that differ from linear trends. Figure 9 (top) represents the oscillatory component detected in standardized stationary annual ST time series for West Siberia. In contrast to the standardized nonstationary ST time series (Figure 8), Figure 9 shows an attenuation of the amplitude with depth. However, the amplitude of the oscillation becomes higher than even the corresponding oscillation in the SAT time series (Figure 8, top). This suggests a relationship between the amplitude of the SSA-detected oscillation and the proportion of variance associated with this component. In fact, the variance of the 7.7 year oscillation is equal to 34, 28, and 45% for the standardized nonstationary time series, and 45, 37, and 50% for the standardized stationary ST time series at depths of 0.4, 1.60, and 3.20 m, respectively. With the linear trend subtracted the proportion of variance associated with the 7.7 year oscillation increases, as does its amplitude.

[55] Another reason for these attenuation and phase shift issues could be our standardization. In general, the variance of the mean ST time series is less than 1.0 and decrease with depth. However, standardization produces a variance of 1.0, i.e., it increases the amplitude of the fluctuation, which, together with a decrease in noise with depth, increases the amplitude of the detected components. Figure 9 shows the trend components detected from nonstandardized annual ST time series for the West Siberia region. As seen from comparing Figures 3a and 9, standardization has an influence on the amplitude of the trend components.

[56] In addition to these potential methodological reasons, we believe that the major explanation for the lack of attenuation with depth and phase shifts is that the physical system does not behave in a purely one-dimensional heat conduction framework. There are a number of very important factors that also affect soil temperature. For instance, the assumption that the ground surface temperature is equal to the 2 m air temperature is likely not true, as there are convective processes, sensible and latent heat fluxes, etc. In fact, STs in the Arctic permafrost regions tend to be 1–2°C higher than the SATs in summer months, and several degrees higher in winter months due to snow insulation effects [*Zhang et al.*, 1997]. Furthermore, snow and vegetation cover greatly complicate this situation, and snow depth has been found to be more important in driving ST than SAT [e.g., *Pavlov*, 1994; *Sokratov and Barry*, 2002; *Frauenfeld et al.*, 2004; *Zhang et al.*, 2005]. This one-dimensional heat conduction also does not incorporate the effects of freeze/thaw processes, such phase changes on the soil thermal regime. Similarly, soil moisture effects are not accounted for. However, our observational soil temperatures are a product of all of these processes, and therefore allow us to, implicitly, account for these processes in a way that modeling exercises cannot easily do. It is reassuring that the observed ST components roughly resemble the modeled ones (Figure 8), but it does not appear that we can observe the same attenuation and phase shifts with depth as would be suggested mathematically. It should be noted that while the detected oscillatory components do not show attenuation in amplitude with depth, the decrease in the proportion of variance associated with these components does testify to their attenuation.

5. Conclusions and Implications

[57] SSA was successfully applied to detect both trend and oscillatory components in ST between 1960 and 1990 over five regions in Russia, and to determine the correspondence between these components in ST and SAT. SSA reconstruction confirms and extends our previous findings on the characteristics of the spatial and temporal responses of ST to SAT increases over Russia [*Chudinova et al.*, 2003]. The trends and oscillatory components in the summer SAT time series correspond to the summer and annual ST time series only over the West Siberia Plain (study region I). In the eastern and western Central Siberian Plateau (regions II and III) and in Transbaikalia (region IV), components reconstructed in the annual ST time series for all depths investigated coincide best with winter ST, even though ST in summer also corresponds well with oscillations of 5–7 year periods in the summer SAT time series.

[58] It must be reiterated that cold season ST oscillations are not only determined by SAT variability. Soil temperature is influenced by other meteorological factors, especially snow depth and seasonal duration of snow cover, as discussed by *Sokratov and Barry* [2002] and *Bartlett et al.* [2004]. However, analysis of the necessary site-specific snow cover data was beyond the scope of this study. SAT

changes alone may be insufficient to account for both short- and long-term changes in ST during the cold season. We find this to be the case for the West Siberian Plain, the eastern Central Siberian Plateau, and the territory east of the Lena River where some of the trend and oscillatory components in winter SAT and ST do not agree.

[59] In the region east of the Lena River (study region V), SSA detected mainly long-term (trend) components and no corresponding oscillations between SAT and ST time series were evident. This may be due to the high degree of ST variability in this region, and hence oscillatory components present in individual time series are lost in the regionally averaged ST time series. In addition, the available number of meteorological stations in region V may be insufficient to adequately characterize such a large territory.

[60] Although we find increasing summer ST in the West Siberia Plain, we believe that this increase does not threaten the region's discontinuous permafrost. The annual ST increase is observed to a depth of 1.6 m only, while the permafrost table in this region is located at 1–2 m [*Yershov*, 1998] and is overlain by deep layers of peat which protect it against warming. A significant increase in annual ST is observed down to a depth of 3.2 m for the Central Siberian Plateau and Transbaikalia. Taking into account the total increase in SAT during the entire 20th century over these territories, the maximum effect on permafrost should be expected in these two regions.

[61] In our previous work [*Chudinova et al.*, 2003] we found the least soil warming between 1969 and 1990 in the territory east of the Lena River, occupied by low-temperature continuous permafrost. The proportion of trend-explained variance in annual ST there is considerably lower than in the other study regions, and the observed rise in ST is also less than that found in the other regions. SAT in the territory east of the Lena River during the last temperature cycle did not exceed the observed highs of the previous cycles. Therefore current warming will not result in the degradation of permafrost in the region east of the Lena River. This conclusion is confirmed by ST measurements in a deep borehole located in the Kolyma lowland (69°52′N, 157°E) where permafrost temperature is stable to depths below 10 m [*Chudinova et al.*, 2003].

[62] The reliability of our results on long- and short-term trend and oscillatory components in ST time series may be limited because of the relatively sparse network of observing stations and the short length of the time series. While we cannot increase the number of stations, we hope to confirm our conclusions once ST data for 1990–2000 have been collected and digitized. This effort is currently underway, and is part of an ongoing collaboration between the National Snow and Ice Data Center at the University of Colorado and the Soil Cryology Laboratory in the Institute of Physicochemical and Biological Problems in Soil Science of the Russian Academy of Sciences.

[63] **Acknowledgments.** We wish to thank the Editor and Associate Editor for their guidance, and we are grateful for the valuable comments provided by Jean-Claude Mareschal and the anonymous reviewers. This work was supported by the North Atlantic Treaty Organization under a grant awarded in 2003 (DGE-0312143), the U. S. National Science Foundation under the Arctic System Science (ARCSS) program grants OPP-0229766 and OPP-0352910, and the International Arctic Research Center (IARC), University of Alaska Fairbanks, under the auspices of NSF cooperative agreement OPP-0327664.

References

Allen, M. R., and L. A. Smith (1994), Investigation of the origins and significance of low-frequency modes of climate variability, *Geophys. Res. Lett.*, *21*, 883–886.

Allen, M. R., and L. A. Smith (1996), Monte Carlo SSA: Detecting irregular oscillations in the presence of colored noise, *J. Clim.*, *9*, 3373–3404.

Anisimov, O. A. (2001), Predicting patterns of near-surface air temperature using empirical data, *Clim. Change*, *50*, 297–315.

Bardin, M. Y. (2002), Air temperature variability over the western areas of Russia and adjacent countries in the 20th century, *Russ. Meteorol. Hydrol.*, *8*, 1–15.

Bartlett, M. G., D. S. Chapman, and R. N. Harris (2004), Snow and the ground temperature record of climate change, *J. Geophys. Res.*, *109*, F04008, doi:10.1029/2004JF000224.

Bartlett, M. G., D. S. Chapman, and R. N. Harris (2005), Snow effect on North American ground temperatures, 1950–2002, *J. Geophys. Res.*, *110*, F03008, doi:10.1029/2005JF000293.

Beltrami, H., and E. Bourlon (2004), Ground warming patterns in the Northern Hemisphere during the last five centuries, *Earth Planet. Sci. Lett.*, *227*, 169–177.

Beltrami, H., and D. S. Chapman (1994), Drilling for a past climate, *New Sci.*, *142*, 36–40.

Beltrami, H., and J. C. Mareschal (1991), Recent warming in eastern Canada: Evidence from geothermal measurements, *Geophys. Res. Lett.*, *18*, 605–608.

Beltrami, H., and J. C. Mareschal (1992), Ground temperature histories for central and eastern Canada from geothermal measurements: Little Ice Age signature, *Geophys. Res. Lett.*, *19*, 692–698.

Beltrami, H., G. Ferguson, and R. N. Harris (2005), Long-term tracking of climate change by underground temperatures, *Geophys. Res. Lett.*, *32*, L19707, doi:10.1029/2005GL023714.

Castagnoli, G. C., S. M. Bernasconi, G. Bonino, P. Della Monica, and C. Taricco (1999), 700 year record of the 11 year solar cycle by planktonic foraminifera of a shallow water Mediterranean core, *Adv. Space Res.*, *24*(2), 233–236.

Chudinova, S. M., S. S. Bykhovets, D. G. Fedorov-Davydov, V. A. Sorokovikov, V. S. Gubanov, R. G. Barry, and D. A. Gilichinsky (2001), Response of temperature regime of Russian north to climate changes during the second half of the 20th century (in Russian), *Kriosfera Zemli*, *5*(3), 63–69.

Chudinova, S. M., S. S. Bykhovets, V. A. Sorokovikov, R. G. Barry, T. Zhang, and D. A. Gilichinsky (2003), Peculiarities in soil warming versus recent climate warming in Russia (in Russian), *Kriosfera Zemli*, *7*(3), 23–31.

Elsner, J. B., and A. Tsonis (1996), *Singular Spectral Analysis: A New Tool in Time Series Analysis*, Springer, New York.

Fallot, J. M., R. G. Barry, and D. Hoogstrate (1997), Variations of mean cold season temperature, precipitation and snow depth during the last 100 years in the former Soviet Union (FSU), *Hydrol. Sci. J.*, *42*, 301–327.

Frauenfeld, O. W., T. Zhang, R. G. Barry, and D. Gilichinsky (2004), Interdecadal changes in seasonal freeze and thaw depths in Russia, *J. Geophys. Res.*, *109*, D05101, doi:10.1029/2003JD004245.

Frauenfeld, O. W., R. E. Davis, and M. E. Mann (2005), A distinctly interdecadal signal of Pacific Ocean–atmosphere interaction, *J. Clim.*, *18*(11), 1709–1718.

Frey, K. E., and L. C. Smith (2003), Recent temperature and precipitation increases in west Siberia and their association with Arctic Oscillation, *Polar Res.*, *22*(2), 287–300.

Gamiz-Fortis, S. R., D. Pozo-Vazquez, M. J. Esteban-Parra, and Y. Castro-Diez (2002), Spectral characteristics and predictability of the NAO assessed through singular spectral analysis, *J. Geophys. Res.*, *107*(D23), 4685, doi:10.1029/2001JD001436.

Ghil, M., and R. Vautard (1991), Interdecadal oscillations and the warming trend in global temperature time series, *Nature*, *350*, 324–327.

Ghil, M., et al. (2002), Advanced spectral methods for climatic time series, *Rev. Geophys.*, *40*(1), 1003, doi:10.1029/2000RG000092.

Gilichinsky, D. A., R. G. Barry, S. S. Bykhovets, V. A. Sorokovikov, T. Zhang, S. L. Zudin, and D. G. Fedorov-Davydov (1998), A century of temperature observations of soil climate: Methods of analysis and long-term trends, in *Proceedings of the 7th International Conference on Permafrost*, edited by A. G. Lewkowicz and M. Allard, pp. 313–317, Univ. Laval, Yellowknife, Northwest Territories, Canada.

Goljandina, N., V. Nekrutkin, and A. Zhigljavsky (2001), *Analysis of Time Series Structure: SSA and Related Techniques*, CRC Press, Boca Raton, Fla.

González-Rouco, F., H. von Storch, and S. E. Zorita (2003), Deep soil temperature as proxy for surface air-temperature in a coupled model simulation of the last thousand years, *Geophys. Res. Lett.*, *30*(21), 2116, doi:10.1029/2003GL018264.

Harris, R. N., and D. S. Chapman (2001), Midlatitude (30–60N) climatic warming inferred by combining borehole temperature with surface air temperature, *Geophys. Res. Lett.*, *28*, 747–750.

Hu, Q., and S. A. Feng (2003), Daily soil temperature dataset and soil temperature climatology of the contiguous United States, *J. Appl. Meteorol.*, *42*(8), 1139–1156.

Huang, S., H. N. Pollack, and P. Y. Shen (2000), Temperature trends over the past five centuries reconstructed from borehole temperatures, *Nature*, *403*, 756–785.

Izrael, Y. A., A. V. Pavlov, and Y. A. Anokhin (2002), Evolution of the cryolithozone under present-day global climate changes (in Russian), *Meteorol. Gidrol.*, *1999*(1), 22–34. (*Russ. Meteorol. Hydrol.*, Engl. Transl., *1999*(1), 14–24, 2002.)

Jevrejeve, S., and J. C. Moore (2001), Singular spectrum analysis of Baltic Sea ice conditions and large-scale atmospheric patterns since 1708, *Geophys. Res. Lett.*, *28*, 4503–4506.

Lachenbruch, A., and B. V. Marshall (1986), Changing climate: Geothermal evidence from permafrost in the Alaskan Arctic, *Science*, *234*, 689–696.

Lewis, T. (1992), Climatic change inferred from underground temperatures, *Global Planet. Change*, *98*, 78–282.

Majorowicz, J. A., and W. R. Skinner (1997), Anomalous soil warming versus surface air warming in the Canadian Prairie Province, *Clim. Change*, *35*, 485–500.

Mann, M. E., and G. A. Schmidt (2003), Ground vs. surface air temperature trends: Implications for borehole surface temperature reconstructions, *Geophys. Res. Lett.*, *30*(12), 1607, doi:10.1029/2003GL017170.

Marcus, S. L., M. Ghil, and K. Ide (1999), Models of solar irradiance variability and the instrumental temperature record, *Geophys. Res. Lett.*, *26*(10), 1449–1452.

New, M. G., M. Hulme, and P. D. Jones (2000), Representing twentieth-century space-time climate variability. Part II: Development of 1901–1995 monthly grids of terrestrial surface climate, *J. Clim.*, *13*, 2217–2238.

Ogi, M., Y. Tachibana, and K. Yamazaki (2003a), Impact of the wintertime North Atlantic Oscillation (NAO) on the summertime atmospheric circulation, *Geophys. Res. Lett.*, *30*(13), 1704, doi:10.1029/2003GL017280.

Ogi, M., K. Yamazaki, and Y. Tachibana (2003b), Solar cycle modulation of the seasonal linkage of the North Atlantic Oscillation (NAO), *Geophys. Res. Lett.*, *30*(22), 2170, doi:10.1029/2003GL018545.

Pavlov, A. V. (1994), Current changes of climate and permafrost in the Arctic and sub-Arctic of Russia, *Permafrost Periglacial Processes*, *5*, 101–110.

Plaut, G., M. Ghil, and R. Vautard (1995), Interannual and interdecadal variability in 335 years of central England temperatures, *Science*, *268*, 710–713.

Pollack, H. N., and D. S. Chapman (1993), Underground records of changing climate, *Sci. Am.*, *268*, 44–50.

Putnam, S. N., and D. S. Chapman (1996), A geothermal climate change observatory: First year results from emigrant pass in northwest Utah, *J. Geophys. Res.*, *101*, 21,877–21,890.

Pollack, H. N., and J. E. Smerdon (2004), Borehole climate reconstructions: Spatial structure and hemispheric averages, *J. Geophys. Res.*, *109*, D11106, doi:10.1029/2003JD004163.

Rasmusson, E. M., X. Wang, and C. F. Ropelewski (1990), The biennial component of ENSO variability, *J. Mar. Syst.*, *1*, 71–96.

Robertson, A. W., and C. R. Mechoso (1998), Interannual and decadal cycles in river flows of southeastern South America, *J. Clim.*, *11*, 2570–2581.

Serreze, M. C., J. E. Walsh, F. S. Chapin III, T. Osterkamp, M. Dyurgerov, V. Romanovsky, W. C. Oechel, J. Morison, T. Zhang, and R. G. Barry (2000), Observation evidence of recent change in the northern high-latitude environment, *Clim. Change*, *46*, 159–207.

Shen, P. Y., and A. E. Beck (1991), Least squares inversion in borehole temperature measurements in functional space, *J. Geophys. Res.*, *96*, 19,965–19,979.

Skinner, W. R., and J. A. Majorowicz (1999), Regional climatic warming and associated twentieth century land-cover changes in north-western North America, *Clim. Res.*, *12*, 39–52.

Sokratov, S. A., and R. G. Barry (2002), Intraseasonal variations in the thermoinsulation effect of snow cover on soil temperatures and energy balance, *J. Geophys. Res.*, *107*(D10), 4093, doi:10.1029/2001JD000489.

Vasiliev, I. S. (1999), Response of Yakutia soil thermal regime to modern climate changes (in Russian), *Meteorol. Gidrol.*, *1999*(2), 98–104. (*Russ. Meteorol. Hydrol.*, Engl. Transl. *1999*(2), 62–66.)

Vasseur, G., and J.-C. Mareschal (1993), La geothermieau service de la paleoclimatologie, *Recherche*, *258*, 1076–1082.

Vautard, R., and M. Ghil (1989), Singular spectrum analysis in nonlinear dynamics, with applications to paleoclimatic time series, *Physica D*, *35*, 395–424.

Vose, R. S., R. L. Schmoyer, P. M. Steurer, T. C. Peterson, R. Heim, T. R. Karl, and J. K. Eischeid (1992), Global Historical Climatology Network: Long-term monthly temperature, precipitation, sea-level pressure, and station pressure data, *Rep. NDP-041*, Carbon Dioxide Inf. Anal. Cent., Oak Ridge Natl. Lab., Oak Ridge, Tenn.

Yershov, E. D. (1998), *General Geocryology*, 580 pp., Cambridge Univ. Press, New York.

Yiou, P., M. Ghil, J. Jouzel, D. Paillard, and R. Vautard (1994), Nonlinear variability of the climatic system, from singular and power spectra of late Quaternary records, *Clim. Dyn.*, *9*, 371–389.

Yiou, P., J. Jouzel, S. Johnsen, and O. E. Rognvaldsson (1995), Rapid oscillations in Vostok and GRIP ice cores, *Geophys. Res. Lett.*, *22*, 2179–2182.

Zhang, T., T. E. Osterkamp, and K. Stamnes (1997), Effects of climate on the active layer and permafrost on the north slope of Alaska, U. S. A., *Permafrost Periglacial Processes*, *8*, 45–67.

Zhang, T., R. G. Barry, D. A. Gilichinsky, S. S. Bykhovets, V. A. Sorokovikov, and J. Ye (2001), An amplified signal of climatic change in soil temperatures during the last century at Irkutsk, Russia, *Clim. Change*, *49*, 41–76.

Zhang, T., et al. (2005), Spatial and temporal variability in active layer thickness over the Russian Arctic Drainage Basin, *J. Geophys. Res.*, *110*, D16101, doi:10.1029/2004JD005642.

R. G. Barry, O. W. Frauenfeld, and T. Zhang, Cooperative Institute for Research in Environmental Sciences, National Snow and Ice Data Center, University of Colorado, 449 UCB, Boulder, CO 80309-0449, USA. (oliverf@colorado.edu)

S. M. Chudinova and V. A. Sorokovikov, Institute of Physicochemical and Biological Problems in Soil Science, Russian Academy of Sciences, Pushchino, Moscow Region 142290, Russia. (chudinova@issp.psn.ru)